(19) Europäisches Patentamt
European Patent Office
Office européen des brevets

(11) EP 3 340 203 A1

(12) EUROPEAN PATENT APPLICATION

(43) Date of publication:
27.06.2018 Bulletin 2018/26

(51) Int Cl.:
G08G 1/01 (2006.01) G08G 1/0967 (2006.01)

(21) Application number: 16205483.7

(22) Date of filing: 20.12.2016

(84) Designated Contracting States:
AL AT BE BG CH CY CZ DE DK EE ES FI FR GB GR HR HU IE IS IT LI LT LU LV MC MK MT NL NO PL PT RO RS SE SI SK SM TR
Designated Extension States:
BA ME
Designated Validation States:
MA MD

(71) Applicant: Bayerische Motoren Werke Aktiengesellschaft
80809 München (DE)

(72) Inventors:
- Rempe, Felix
80336 München (DE)
- Fastenrath, Dr. Ulrich
85399 Hallbergmoos (DE)
- Franeck, Philipp
81667 München (DE)
- Bogenberger, Dr. Klaus
80638 München (DE)

(54) TRAFFIC VELOCITY ESTIMATION SYSTEM

(57) The present invention relates to a computer system for calculating accurate estimations of traffic velocity in a road network. The system comprises a plurality of devices, each device operable to deliver speed measurement data corresponding to the speed of a traffic flow in the road network. The system further comprises at least one computational unit, wherein each of the plurality of devices sends speed measurement data to the computational unit. The computational unit is operable to calculate accurate estimations of traffic velocity in the road network for specific regions by identifying regions with varying sizes and moving boundaries under the condition that within each region, a corresponding traffic phase p is constant, wherein each traffic phase is one of a free-flow phase, a synchronized phase or a wide moving jam phase; and calculating accurate estimations of traffic velocity in said regions based on the corresponding traffic phases.

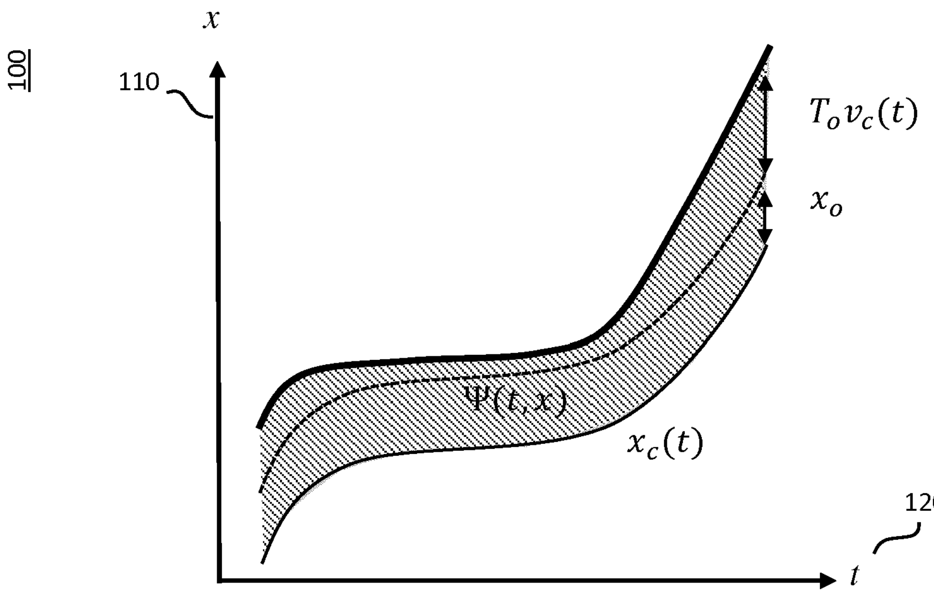

Fig. 1A

EP 3 340 203 A1

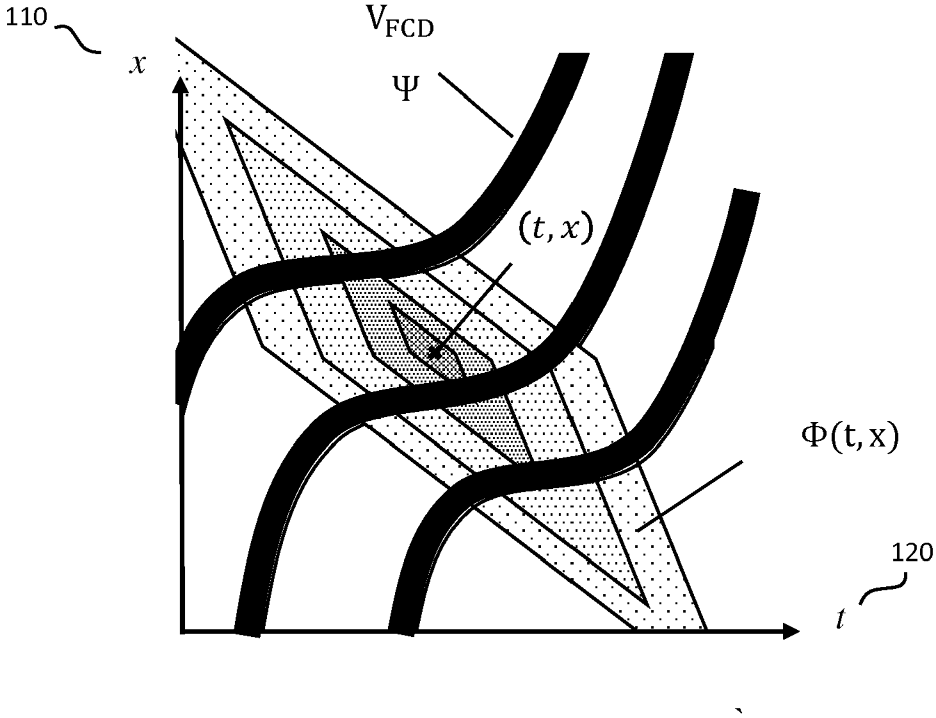

Fig. 1B

Description

[0001] The present invention relates to a system and method for accurate traffic velocity estimations.

[0002] Modern navigation systems in vehicles include traffic flow estimation in order to provide users of vehicles with an estimated travel time for a particular route the user wants to take. However, traffic flow estimation is inaccurate and cumbersome since generally, only a limited number of sensors is available that provide sparse measurements of a real traffic situations in space and time. The main task in estimating the traffic flow is in processing these measurements and providing an estimate of a desired traffic variable for every position on a road and every point in time with the goal to reconstruct prevailing real traffic conditions most accurately.

[0003] In recent years, the availability of Floating Car Data (FCD) or other speed measurement data corresponding to the speed of a traffic flow in the road network has quickly spread and is increasingly available for traffic flow estimation in a road network. Using FCD is advantageous since it provides the possibility to obtain traffic data on each position along a road network. Besides this highly spatial resolution of available data, another advantage of FCD is the ever-decreasing cost of retrieving said data such that FCD will be further increasingly available in the future. However, time intervals between two reported trajectories in a road segment of the road network can vary strongly. In addition, FCD usually do not explicitly contain traffic state data - e.g. data on a traffic density (traffic density data) and/or a traffic flow (traffic flow data). Further, FCD is generally only sparsely available over the vehicle network. This sparsity of FCD and non-availability of traffic state data coupled with high spatiotemporal traffic dynamics along the road network are a major challenge for accurate traffic estimations.

[0004] To address the above problems, traffic flow estimation approaches have been introduced that take into consideration traffic dynamics. Said traffic flow estimation approaches can be classified into two categories. The first category comprises analytical flow models coupled with data assimilation techniques. However, in practice, said traffic flow estimation approaches require traffic state data (i.e. traffic flow data and traffic density data) in addition to FCD, thereby limiting the applicability in large scale since it adds further complexity to data acquisition and data processing for traffic flow estimation. The second category of traffic flow estimation comprises estimation methods based on empirical traffic theory. In particular, one approach uses FCD for estimating velocities in the road network by classifying traffic on the road network into one of the following traffic phases: free-flow-phase, synchronized flow phase and wide moving jam phase. A major drawback, however, is that velocities within the traffic phases are estimated as constant over space and time. Doing so strongly limits the accuracy of the said traffic phase estimations. Other methods belonging to the second category of approaches apply basic filtering operations to measured data. They tend to unconditionally propagate low velocities up- and downstream although low velocities might be part of stationary congestion upstream a bottleneck. Hence, when only sparse probe data is available, the estimated velocities in stationary congestion patterns lack accuracy.

[0005] Therefore, it is an object of the present invention to overcome the above-mentioned drawbacks by accurately estimating traffic velocity along a road network based on sparse probe data as input.

[0006] This problem is solved by the independent claims. Preferred embodiments are described in the dependent claims.

[0007] According to a first aspect, a computer system for calculating accurate estimations of traffic velocity in a road network, the system comprising:

a plurality of devices, each device operable to deliver speed measurement data corresponding to the speed of a traffic flow in the road network; and
at least one computational unit,
wherein each of the plurality of devices sends speed measurement data to the computational unit, and
wherein the computational unit is operable to calculate accurate estimations of traffic velocity in the road network by:

- identifying regions with varying sizes and moving boundaries under the condition that within each region, a corresponding traffic phase p is constant, wherein each traffic phase is one of a free-flow phase, a synchronized phase or a wide moving jam phase;
  and
- calculating (230) accurate estimations of traffic velocity in said regions based on the corresponding traffic phases.

[0008] The at least one device may be e.g. an external device, e.g. a mobile device, which is assigned to a particular vehicle. E.g. the mobile device may be a smart phone that may run an appropriate application, app, providing the functionality to send the speed measurement data to the computational unit. The mobile device may send the speed measurement data to the computational unit e.g. whenever a connection allowing data transfer (e.g. Bluetooth, etc.) is established with the vehicle and the vehicle sends a notification to the device that it is in a driving mode.

[0009] The computational unit may be a backend server. Alternatively or additionally, the computational unit may (at least partly) be located in a vehicle. Alternatively or additionally, the computational unit may be part of the road infrastructure corresponding to the road network.

The at least one device may alternatively or additionally be a device integrated into the vehicle and providing the respective functionality for sending the speed measurement data, e.g. a navigation unit of the vehicle.

[0010] Alternatively or additionally, the at least one device may be a traffic sensor located along a road in the road network operable to assess speed measurement data of vehicles passing the traffic sensor

[0011] Alternatively or additionally, the at least one device may be integrated into a vehicle on the road providing speed measurement data of at least one other vehicle that is in the proximity of the vehicle the device is assigned to.

[0012] Alternatively or additionally, the at least one device is a mobile device assessing speed measurement data of vehicles from above the road, e.g. a satellite, airplane, helicopter, quadrocopter.

[0013] The speed measurement data may be sent when the vehicle is in a driving mode periodically, e.g. every 2 second (s), every 5 s, every 10s, every 20s, every 30s, or any other appropriate period of time for sending the speed measurement data. In the example where the at least one device is or comprises an external device (cf. above) or is integrated into the vehicle, the speed measurement data may be floating car data, FCD. In the example where the at least one device is or comprises a traffic sensor, the speed measurement data may be sent each time a vehicle passes the traffic sensor. Alternatively, the external sensor measures the speed of a predetermined amount of vehicles passing the traffic sensor, calculate an average speed of the vehicles and send the calculated average speed as speed measurement data to the computational unit. The terms FCD and speed measurement data will be used interchangeably hereinafter.

[0014] Each region is defined as a part of a road segment of length *L*, wherein the size and the boundaries of said region may change over time. Over time, said region may further divide into two or more regions, or two or more regions may merge into one region.

[0015] A road network may be a system of interconnecting lines and points (edges and nodes) that represent a system of streets or roads. The road network may be divided into one or more road segments. Further definitions for road network, road segment and region are provided below.

[0016] Especially in view of the vehicles supporting an autonomous driving mode, the accurate estimation of traffic velocity is no longer just a tool for estimating a travel time for a particular route to a driver, but rather represents important data for road safety in view of improving the autonomous driving mode. In particular, on the one hand, each vehicle operating in an autonomous driving mode may use the data/information for determining a best route to a destination (e.g. if the velocity is rather low on one route, an alternative route with a better velocity may be autonomously chosen by the vehicle). On the other hand, the data/information on the velocity may be used in order to improve the security of all traffic participants in the road network, since the velocity data may be used by autonomous vehicles and/or by navigation systems of any vehicles to foresee road segments with low velocity and adapt the driving behavior accordingly.

[0017] According to an embodiment,

each speed measurement data comprises at least a location of a vehicle driving on the road network and a corresponding timestamp; and

wherein each speed measurement data may further comprise:

- a velocity of the vehicle at a point in time corresponding to the timestamp;
- a direction of the vehicle at the point in time corresponding to the timestamp;
- a lane the vehicle is driving on; and/or

data on vehicles and their velocities surrounding the vehicles.

[0018] Each location of the vehicle may comprise a position of the vehicle at the road network. Each position may be obtained using navigation satellite systems comprising Global Positioning System (GPS), GLObal Navigation Satellite System (GLONASS), Galileo positioning system, and BeiDou Navigation Satellite System. In particular, each position may be obtained from a respective module located in the vehicle. In the example of the Global Positioning System, each GPS - position that may be determined by a GPS-Module located in the vehicle. In this example, each speed measurement data may comprise a current GPS-Position of the vehicle. Since the vehicle (or the device corresponding to the vehicle) transmits speed measurement data comprising corresponding GPS-data to the computational unit, the computational unit may track the position of the vehicle and determine position x along a corresponding road segment as part of the road network with $x \in [0, L]$. Each timestamp may correspond to a particular point in time t the vehicle was at the respective position x along the road segment. The GPS-Module may be located in the external device and in the traffic sensor, respectively (cf. above).

[0019] The velocity of the vehicle may be calculated from the speed measurement data, as is explained in more detail below, or may be obtained from a speed sensor as e.g. located in the vehicle and/or in the traffic sensor.

[0020] The direction of the vehicle c may be calculated from the speed measurement data or determined from a direction sensor that may be located in the vehicle.

[0021] The lane the vehicle is currently driving on may be determined from further sensors, e.g. one or more cameras located in and/or on the vehicle and/or at the traffic sensor.

[0022] The data on vehicles and their velocities surrounding the vehicle (sending the speed measurement data) may be determined from further sensors, e.g. cameras, RAdio Detection And Ranging (RADAR) sensors, Light Detection And Ranging (LIDAR) sensors, photo sensors, thermal imaging cameras located in and/or on the vehicle, and/or any further appropriate sensors for providing the appropriate data.

[0023] According to a further embodiment, identifying the regions comprises:

- calculating, from the speed measurement data, criteria probabilities $P_p^i(t,x)$ for each traffic phase *p*;
- calculating, as the product of all criteria probabilities, the independent probability $P_p'(t,x)$ for each traffic phase *p*;
- estimating the uncertainty probability $P_U \in [0,1]$, wherein P_U describes a level of uncertainty in assigning (t, x) to any of the phases p;
- taking into account the dominance of the wide moving jam phase; and
- determining final phase probabilities P_p;

wherein P denotes probability; and p denotes phase.

[0024] According to a further embodiment, calculating criteria probabilities P_p^i comprises the following: let $P_p^1, P_p^2, \ldots, P_p^{N_k}$, $P_p^i \in \mathbb{R}$ be $N_k(p) \in \mathbb{N}\backslash\{0\}$ criteria that (*t*, *x*) needs to fulfill in order to belong to phase p, wherein each criterion is modelled as a fuzzy decider $P_p^i \in [0,1].$

[0025] According to a further embodiment, the independent probability $P_p'(t,x)$ for each traffic phase p is calculated as follows:

$$P_p'(t,x) = \prod_i^{N_k(p)} P_p^i(t,x).$$

[0026] According to a further embodiment, the uncertainty probability $P_U \in [0,1]$ that describes the probability that (*t*, *x*) does not belong to any of the phases Ω is calculated by:

$$P_U(t,x) = \Pi_{p\in\Omega}\left(1 - P_p{}'(t,x)\right).$$

[0027] According to a further embodiment, if there is an occurrence of a high probability of a region belonging to $(P_J'$ and $(P_S{}'$ or $P_F'))$, the dominance of P_J' is taken into account.

[0028] According to yet a further embodiment, determining the final phase probabilities *Pp* while taking into account the dominance of P_J' for each region is performed as follows:

$$P_J(t,x) = P_J{}'(t,x)$$

$$P_S(t,x) = P_S'(t,x) \cdot (1 - P_J(t,x))$$

$$P_F(t,x) = P_F'(t,x) \cdot (1 - P_J(t,x)).$$

[0029] According to a further embodiment, calculating accurate estimations of traffic velocity based on a prevailing traffic phase in the road network comprises:

estimating phase-dependent velocity estimates $V_p^H(t,x);$ and

aggregating final-phase probabilities P_p and corresponding velocity estimates $V_p^H(t,x)$ into velocity estimates V_E.

[0030] According to a further embodiment, estimating phase-dependent velocity estimates $V_p^H(t,x)$ comprises:

$$V_p^H(t,x) = \frac{1}{V_{V_{FCD}^{-1}}(P_p, \Phi_p^H, t, x)};$$

with $V_{V_{FCD}^{-1}}(\mathrm{P_p}, \Phi_\mathrm{p}^\mathrm{H}, \mathrm{t}, \mathrm{x})$ denoting a convolution process smoothing the inverted trajectory velocities $V_{V_{FCD}^{-1}}$ with the convolution kernel Φ_p^H.

[0031] According to another embodiment, aggregating final-phase probabilities P_p and the corresponding velocity estimates $V_p^H(t,x)$ into velocity estimates V_E comprises:

$$V_E(t,x) = \frac{P_U(t,x) \cdot V_U(t,x) + \sum_{p \in \Omega} P_p(t,x) \cdot V_p^H(t,x)}{P_U(t,x) + \sum_{p \in \Omega} P_p(t,x)};$$

with V_U = a speed limit of the respective region.

[0032] According to yet another embodiment, at least one of the vehicles driving on the road network supports an autonomous driving mode;
wherein the computational unit is further operable to send the accurate estimations of traffic velocity to the vehicle supporting an autonomous driving mode; and
wherein the vehicle supporting the autonomous driving mode is operable to take the accurate estimations of traffic velocity into account when operating in the autonomous driving mode.

[0033] Vehicles comprising/supporting an autonomous driving mode for (at least in part) autonomously transporting passengers form one location to another are known. However, the autonomous driving mode is not yet available in a fully automated manner. Some vehicles require periodic input from an operator, e.g. a driver or passenger, whereas other vehicles and/or the driver of the vehicle may switch from a manual to an autonomous mode and vice versa, whenever applicable and/or allowable. In order to improve the security and efficiency of autonomous driving modes, the computational unit may send the accurate estimations of traffic velocity to all vehicles supporting an autonomous driving mode and previously registered via an appropriate application to the computational unit. Hence, the vehicles may use the accurate estimations of traffic velocity to the vehicles which may be taken into account of the respective vehicles for the autonomous driving mode. The security and efficiency of the autonomous driving mode is hence greatly improved. Alternatively and/or additionally, the computational unit may send the accurate estimations of traffic velocity to each vehicle previously registered at the computational unit, irrespective of whether the vehicle supports an autonomous driving mode. In this example, a navigation module of the vehicle may take the accurate estimations of traffic velocity into account for planning trips, warning drivers from jams and accurately predicting a time of arrival.

[0034] According to another aspect, a computer-implemented method for calculating accurate estimations of traffic velocity in a road network is provided, the method comprising:

sending, by a plurality of devices, speed measurement data to a computational unit, wherein each speed measurement data corresponds to the speed of a traffic flow in the road network,
and
calculating, by the computational unit, accurate estimations of traffic velocity in the road network by:

- identifying regions with varying sizes and moving boundaries under the condition that within each region, a corresponding traffic phase *p* is constant, wherein each traffic phase is one of a free-flow phase, a synchronized phase or a wide moving jam phase; and
- calculating accurate estimations of traffic velocity in said regions based on the corresponding traffic phase.

[0035] According to another aspect, a computer program product is provided comprising instructions thereon, which, when loaded and executed by at least one processor, cause the at least one processor to perform a method according to claim 13.

[0036] The aspects defined above and further aspects of the present invention are apparent from the examples of embodiment to be described hereinafter and are explained with reference to the examples of embodiment. The invention will be described in more detail hereinafter with reference to examples of embodiment. However, it is apparent to the person skilled in the art that the invention is not limited to the examples of embodiment.

Figure 1A shows an area $\Psi(t, x)$ represented by a space interval $[x_c(t), x_c(t) + x_0 + T_0 \cdot v_c(t)]$ of one vehicle at time t;

Figure 1B shows a smoothing operation on FCD;

Figure 2 shows steps performed for estimating accurate velocities in a road network;

Figure 3 shows results of the sigmoid functions parameterized for free flow, synchronized flow and WMJ;

Figure 4 shows raw trajectory data for a road segment;

Figure 5 shows a computation of the final phase probabilities P_P, the phase-dependent velocity estimates V_p^H, the final velocity estimate V_E and an estimate of the quality of the estimate denoted as $(1-P_U)$

Figure 6 shows obtained estimation results applying three approaches PSM, GASM and naïve; and

Figure 7 shows the MAPE with respect to data densities between 10 traces/hour and 90 traces/hour for the naïve approach, the GASM approach and the PSM approach.

Definitions

[0037] A road network may be a system of interconnecting lines and points (edges and nodes) that represent a system of streets or roads. The road network may be divided into one or more road segments. For example, each line (edge) between two interconnecting points (nodes) may be a road segment. However, the road network may be divided into road segments in any other appropriate manner. Moreover, traffic on each road segment may be divided into three traffic phases. The first traffic phase is the free flow phase (in the following also referred to as: free flow). The free flow describes a state of traffic where traffic flow and traffic density are nearly in a linear relation. In the free flow, traffic demand is lower than a capacity of the respective road segment. Therefore, there may exist a high spread of velocities between vehicles driving on different lanes of the road segment. The average velocity in free flow can be estimated to greater than or equal (≥) 65 km/h (kilometers per hour) for roads with a speed limit greater of equal 85km/h or roads with unlimited speed limit.

[0038] The second traffic phase is the synchronized flow phase (also referred to hereinafter as: synchronized) is characterized by high vehicle densities. In particular, the traffic demand corresponds to the capacity of the respective road segment. The average velocity of vehicles in synchronized flow is significantly lower than the average velocity of vehicles in free flow and can be estimated between 30km/h and 65 km/h. Further, the variance of velocities among vehicles on different lanes of the road segment is lower than the variance of velocities in free flow traffic. A transition from free flow to synchronized flow can appear spontaneously on each road segment, e.g. due to local perturbations such as lane changing maneuvers and/or can be induced by moving jams propagating upstream. A transition from free flow to synchronized flow may infer a drop in the road capacity, e.g. at a bottleneck (e.g. an on/off-ramp), a closure of a lane and/or a beginning of a constructions site. When a maximum road capacity reduces and the traffic demand does to significantly change, the synchronized traffic phase may persist.

[0039] The third traffic phase is the Wide Moving Jam (WMJ) - phase (in the following also referred to as WMJ). The average velocity (hereinafter also referred to as mean velocity) in the WMJ can be estimated to lower than or equal (≤) 30 km/h. The WMJ may occur spontaneously, e.g. when a vehicle in a synchronized decelerates stronger than necessary, resulting in a shockwave that propagates upstream (i.e. backwards from the decelerating vehicle) forming an upstream front of a WMJ. In synchronized flow, i.e. when vehicle density is high, it is likely that an over-deceleration happens. In this case, the average velocity can decrease down to 0 km/h.

[0040] A trajectory of a vehicle $c \in \{1, ..., N_c\}$ with N_c = a total number of vehicles (each vehicle corresponding to floating car data received at the computational unit), is a function $x_c(t) \in [0, L]$ denoting a position of vehicle c along a road segment with length $L \in \mathbb{R}_+$ at time t.

[0041] Each road segment is a predefined part of the road network starting with a length unit (e.g. in m, km or any other appropriate unit of length) count of 0 and ending with length $L \in \mathbb{R}_+$. An exemplary road segment is shown in **Figure 4**, cf. 420.

[0042] Accordingly, the derivative of the function $x_c(t)$ with respect to the time, $v_c(t)$, is the velocity of vehicle c at time (point in time) t.

[0043] Each vehicle c passes a space-time domain $[0, L] \times [0, T]$ of a road segment with length L, observed for time period T, provides information about a part of the space-time domain.

[0044] x_0 is the sum of a length of vehicle c (e.g. in centimeter cm, meter m, or any other appropriate unit of length representing the length of c) and a minimal distance to the preceding vehicle in queueing traffic. The minimal distance to the preceding vehicle in queueing traffic may be a constant, e.g. 1 m, 1.5m, 2m, 2.5m, 3m, 3.5 m or any other constant representing an appropriate or mandatory minimal distance to the preceding vehicle in queuing traffic.

[0045] A "minimal space gap" is a non-constant space gap between a first vehicle to a preceding second vehicle that increases linearly with velocity $v_c(t)$ depending on time headway T_0, wherein time headway T_0 is an elapsed time between a first point in time the preceding second vehicle finishes passing a fixed point at the road segment and the first vehicle starts to pass that fixed point at the road segment.

The PSM-approach

[0046] The present approach presented within this application is also referred to as novel Phase-based Smoothing Method (PSM) approach.

[0047] In view of the above definitions, **Figure 1 A** shows an area $\Psi(t, x)$ (also referred to as area or area Ψ) represented by space interval $[x_c(t), x_c(t) + x_0 + T_0 \cdot v_c(t)]$ at time t that vehicle c occupies. The occupied area Ψ represented by space interval $[x_c(t), x_c(t) + x_0 + T_0 \cdot v_c(t)]$ in space-time (t, x) signifies that in this area Ψ, only one vehicle c can exist on a single-laned road. Further, it is assumed that the vehicle's velocity is a representation of the traffic velocity in the occupied area.

[0048] In other words, area $\Psi(t, x)$ is a function that indicates whether at time t 120, position x 110 (wherein x 110 is an arbitrary position along the road segment with $x \in [0, L]$) is occupied by *any* observed vehicle c:

$$\Psi(t,x) = \begin{cases} 1 & \text{if } \exists c: x_c(t) < x < x_c(t) + x_0 + T_0 v_c(t) \\ & 0 \text{ else} \end{cases} \tag{1}$$

with 1 = true (i.e. at time t 120, position x 110 is occupied) and 0 = false (i.e. at time t 120, position x 110 is not occupied), wherein

$\Psi(t, x)$ has the following properties:

(a) if traffic density is high, all vehicles c keep a time headway of T_0 to their preceding vehicles and all vehicle positions $x \in [0, L]$ at the road segment as well as velocities are known, then $\Psi(t, x) = 1$, $\forall t \in [0, T]$, $x \in [0, L]$.

(b) if traffic density is low and gaps between vehicles are high, there are times and positions where $\Psi(t, x) = 0$;

(c) if only for a part of all existent vehicles c their trajectories and velocities are known, then occupied part decreases the smaller the penetration rate of observed vehicles c.

[0049] Accordingly, $V_{FCD}(t,x) \in \mathbb{R}_+$ denotes the velocity data $v_c(t)$ reported by all (devices located in the corresponding) vehicles c combined into a single, two-dimensional function. This velocity is only valid in space-time (t, x) which is occupied by any vehicle c^* (i.e. area $\Psi(t, x) = 1$), and is set to the velocity of the closest vehicle upstream of (t, x):

$$\mathrm{V}_{FCD}(t,x) = \begin{cases} v_{c^*}(t) \ \text{ if } \Psi(t,x) = 1, c^* = \underset{\forall c: x - x_c(t) \geq 0}{\operatorname{argmin}} (x - x_c(t)) \\ \qquad -1 \text{ else} \end{cases} \tag{2}$$

[0050] In order to process data locally, the two-dimensional convolution is a common and often used operation. The function

$$\Gamma_{\mathrm{V_{FCD}}}(\mathrm{w}, \Phi, \mathrm{t}, \mathrm{x}) = \int_0^T \int_0^L \Phi(t - \hat{t}, x - \hat{x}) \cdot w(\hat{t}, \hat{x}) \cdot V_{FCD}(\hat{t}, \hat{x}) \cdot \Psi(\hat{t}, \hat{x}) \, d\hat{x} d\hat{t} \tag{3}$$

represents a *weighted* continuous convolution. $\phi(t,x) \in \mathbb{R}$ denotes a kernel function and $w(t,x) \in \mathbb{R}$ a space-time-dependent weight of the input data, in this case the velocity measurements V_{FCD}. Definitions of kernel functions and weightings are given further below. In order to use the convolution equation for smoothing operations, results of $\Gamma_{V_{FCD}}$ need to be normalized. The normalization term is similar to the aforementioned convolution but omits velocity input V_{FCD}:

$$D(\mathrm{w}, \Phi, \mathrm{t}, \mathrm{x}) = \int_0^T \int_0^L \Phi(t-\hat{t}, x-\hat{x}) \cdot w(\hat{t}, \hat{x}) \cdot \Psi(\hat{t}, \hat{x})\, d\hat{x} d\hat{t} \quad (4)$$

[0051] Later, applied kernel $\Phi(t, x)$ and weighting $w(t, x)$ are chosen in such away that $D(w,\Phi,t,x)$ represents an estimate of the data density in the regions. The normalized convolution of weighted and velocity function $V_c(t, x)$ with kernel $\Phi(t, x)$ is then stated as:

$$V_{V_{FCD}}(w, \Phi, t, x) = \frac{\Gamma_{\mathrm{V_{FCD}}}(w,\Phi,t,x)}{D(w,\Phi,t,x)} \quad (5)$$

[0052] For example, given a kernel function that returns only positive/zero values and has its maximum at (0,0), eq. (5) describes a common smoothing process, as depicted in **Figure 1B**. Then, for space-time (t, x) a weighted average velocity of all nearby velocities is computed (that are inside the occupied area $\Psi(t, x)$), where the weights depend on their distance to (t, x).

[0053] The convolution kernel Φ allows a great variety of operations in general. Within the scope of the present subject-matter, the convolution kernel Φ is used for smoothing operations. For traffic related smoothing with characteristic wave speeds, the following simple and effective kernel formulation is also adopted here:

$$\Phi_{\mathrm{v_{dir}}}^{\tau,\sigma}(t,x) = \begin{cases} \exp\left(-\left|\frac{t-\frac{x}{v_{dir}}}{\tau}\right| - \left|\frac{x}{\sigma}\right|\right) & \text{if } v_{dir} \neq 0 \\ \exp\left(-\left|\frac{t}{\tau}\right| - \left|\frac{x}{\sigma}\right|\right) & \text{if } v_{dir} = 0 \end{cases} \quad (6)$$

It defines a main smoothing direction v_{dir} that is used in order to interpolate velocities in a characteristic direction of shockwaves v_{dir} (see (16) for more details). Its maximal value is located at (0*s*, 0*m*) and function values decay exponentially toward zero. In **Figure 1B**, a kernel with negative velocity v_{dir} is depicted exemplarily as a discrete contourplot. Note that Φ is actually a continuous function.

[0054] **Figure 2** shows the steps 200 performed for estimating accurate velocities V_E 230 in the road network. These steps are performed using floating car data, FCD, but, however, may also be performed using any kind of speed measurement data. In particular, it is shown how the FCD (hereinafter also referred to as 'raw trajectory data') V_{FCD} 210 is estimated into a continuous velocity estimate $V_E(t, x)$.

[0055] First, a calculation of final phase probabilities P_P is performed 220.

[0056] Let $\Omega = \{F,S,J\}$ be the set of the phases 'Free Flow' (F), 'Synchronized Flow' (S) and 'Wide Moving Jam'; also referred to as 'WMJ' (J) (as outlined above). Then, $P_p(t, x) \in [0,1]$ with $p \in \Omega$ denotes the probability for the traffic at time t and at position x to be in phase p.

[0057] In a first step, the FCD (also referred to herein as raw trajectory data) 210 is convolved with different smoothing kernels (cf. above, and equation (13)), resulting in smoothing data. Resulting values are evaluated to what extent they fulfill several fuzzy phase criteria. Respective criteria probabilities $P_p^i\,(t,x)$ denote the degree of fulfillment 221 at space-time *(t, x)*. As described above, each traffic phase has different empirical characteristics, such as the aforementioned velocity ranges and respective traffic densities and traffic flows. The free flow phase has low traffic densities and high velocities, the synchronized flow phase lower velocities and higher densities and the Wide Moving Jam phase highest traffic densities and lowest velocity ranges. These empirical characteristics can be used in order to identify the phase *p* each space-time *(t, x)* probably belongs to. Let $P_p^1, P_p^2, \ldots, P_p^{N_k}$, $P_p^i \in \mathbb{R}$ be $N_k(p) \in \mathbb{N}\backslash\{0\}$ criteria that (t, x) needs to fulfill in order to belong to phase p. Each criterion is modelled as a fuzzy decider $P_p^i \in [0,1]$.

[0058] In a next step, the independent probability $P_p'(t,x)$ is determined 222 as the product of all criteria probabilities for each phase individually:

$$P_p'(t,x) = \prod_{i}^{N_k(p)} P_p^i(t,x) \quad (7)$$

[0059] For each phase, different criteria are aggregated into preliminary phase probabilities P_p'. Consequently, the preliminary phase probability P_p' is always lower or equal to the lowest criteria probability P_p^i. In other words that means that all criteria need to be fulfilled to a certain degree in order to assign a point in space-time to phase *p*. A specific example for two different criteria is provided in more detail with respect to Table 1 below.

[0060] In a next step, probability $P_U \in [0,1]$ is estimated 223, which describes the level of uncertainty in assigning (*t, x*) to any of the phases. In other words P_U describes the probability that (*t, x*) does not belong to any of the phases:

$$P_U(t,x) = \Pi_{p\in\Omega}\left(1 - P_p{}'(t,x)\right) \quad (19)$$

[0061] For space-time *(t, x)* where the uncertainty is high a best-guess velocity V_U needs to be assumed. The speed limit may be the best-guess velocity V_U. In another example, other kinds of velocities, e.g. historical averages, may be the best guess velocity V_U.

[0062] Then, the dominance of the J-phase (WMJ-phase) is taken into account 224. Since P_p' are independent, regions may occur especially in the presence of shockwaves, where both P_J' and $(P_S{}' \text{ or } P_F')$ estimate high probabilities. That is due to the different shapes of the convolution kernels and according velocities that are considered for the determination of the phase. Since WMJs can propagate through other phases without interruption (cf. equation (14)), plus, probability P_J' is supported by more distinctive criteria, it is reasonable to assume that these regions rather belong to the J phase than to one of the others. Consequently, in those cases dominance of the J phase over the other phases is determined.

[0063] Finally, the final phase probabilities P_p are determined 225, taking into account the dominance of the J phase by:

$$P_J(t,x) = P_J{}'(t,x) \quad (20)$$

$$P_S(t,x) = P_S'(t,x) \cdot (1 - P_J(t,x)) \quad (21)$$

$$P_F(t,x) = P_F'(t,x) \cdot (1 - P_J(t,x)) \quad (22)$$

[0064] Based on these and raw trajectory data, for each phase and each point in space-time a velocity estimate $V_p^H(t,x)$ is computed 231. Additionally, a *fallback* velocity $V_U(t, x)$ is assumed that serves as a best-guess velocity in case the uncertainty P_U is high. The fallback velocity (also referred to herein as best-guess velocity) may be a speed limit. In another example, the fallback velocity may be a historical average velocity or any other appropriate velocity.

[0065] Finally, the resulting estimate $V_E(t, x)$ is determined 232 by aggregating the probabilities $P_p(t, x)$ and $P_U(t, x)$ and their respective velocity estimates $V_p^H(t,x)$ and $V_U(t, x)$.

[0066] The above steps are explained in the following example that is provided with respect to **Table 1**.

[0067] <u>Calculation of criteria probabilities P_p^i 221</u>

[0068] For the sake of simplicity, an example is provided where two classes of criteria P_p^1, P_p^2 are presented and later applied. However, it is clear to the person skilled in the art that the design of the approach allows the usage of a more than two criteria. In particular, further criteria might be used in order to further distinguish between phases $p \in \Omega$ with $\Omega = \{F,S,J\}$. For example, if flow or density information is available that can be used in order to further differentiate between phases p by designing dedicated criteria. In addition to or alternatively, prior bottleneck data could be integrated into the procedure. If there are known bottlenecks, for the regions upstream of that bottleneck along the road segment, a prior probability as congested flow could be assigned. In this example, the approach would constitute a fusion of real data and expected congested regimes.

[0069] First Class of Criteria P_p^1

[0070] Back to the example: the first criterion is a velocity criterion P_p^1 that uses velocity data of smoothed data for determining the phase probability. The second is a density criterion P_p^2. The density criterion P_p^2 is applied to ensure that a phase hypothesis is supported by nearby data. In this context density refers to the data or, in other word, the number of velocity measurements nearby.

Table 1

	Velocity Criterion P_p^1	Density Criterion P_p^2	Preliminary Phase Probability	Final Phase Probability
Free Flow	P_F^1	P_F^2	$P_F' = P_F^1 \cdot P_F^2$	$P_F = P_F' \cdot (1 - P_J')$
Synchronized Flow	P_S^1	P_S^2	$P_S' = P_S^1 \cdot P_S^2$	$P_S = P_S' \cdot (1 - P_J')$
Wide Moving Jam	P_J^1	P_J^2	$P_J' = P_J^1 \cdot P_J^2$	$P_J = P_J'$
Uncertain State			$P_U = (1 - P_F')(1 - P_S')(1 - P_J')$	

[0071] The velocity of vehicle c at time t $v_c(t)$ (herein also referred to as: 'velocity data') represents very important data for accurately determining to which traffic phase space-time *(t, x)* probably belongs to. The underlying idea of this criterion is to use velocity data measured in phase-characteristic directions around *(t, x)* and determine probability P_p^1. It is known that each transition from free flow to congested flow (in the following also referred to as: traffic breakdown) is a probabilistic event triggered by perturbations. A traffic breakdown is usually connected to a capacity drop of the road infrastructure and a significant drop in average velocities. Consequently, velocity suits well to distinguish between free flow and congested flow. In order to differentiate between free flow and congested flow, fuzzy thresholds v_F^{thres} and v_S^{thres} are applied.

[0072] The distinction between WMJ and synchronized as congested regimes is less obvious. In fact, the upper velocity of the WMJ is significantly smaller than the threshold to free flow. As outlined above, velocities in WMJ can decrease down to 0km/h, such that no lower bound is required.

[0073] A fuzzy decider function $\sigma(v, v^{thres}, \lambda)$ (sigmoid function, i.e. a bounded differentiable real function that is defined for all real input values and has a positive derivative at each point) is applied that translates a velocity v into a probability $P_p^1 \in [0,1]$. Parameters are threshold v^{thres} and λ determining the strictness of the threshold. In other words, the higher λ, the higher the gradient of the transitionsection:

$$\sigma(v, v^{thres}, \lambda) = 1 - \frac{1}{1+\exp\left(-\lambda\left(v - v^{thres}\right)\right)} \tag{8}$$

[0074] Figure 3 shows the results of the sigmoid functions parameterized for free flow 310, synchronized flow 320 and WMJ 330 with respect to different velocities.

[0075] Probabilities $P_F^1(t, x)$ and $P_S^1(t, x)$ are computed as follows:

$$P_F^1(t,x) = 1 - \sigma\left(V_F(t,x), v_F^{thres}, \lambda_F\right) \quad (9)$$

$$P_S^1(t,x) = \sigma\left(V_S(t,x), v_S^{thres}, \lambda_S\right) \quad (10)$$

[0076] Where v_p^{thres} and λ_p denote the parameters of the decider function with respect to the characteristic velocity ranges of the phase *p*. The velocities V_F and V_S are computed according to the normalized convolution process equation (5) as:

$$V_F(t,x) = V_{V_{FCD}}(w^0, \Phi_F, t, x) \quad (11)$$

$$V_S(t,x) = V_{V_{FCD}}(w^0, \Phi_S, t, x) \quad (12)$$

with Φ_F and Φ_S denoting phase specific smoothing kernels, with characteristic speeds of v_p^{dir} and parameters τ_p and σ_p. w^0 denotes a standard weighting where $w^0(t, x) = 1$. The standard weighting implies that all smoothed raw data have an equal significance for the determination of the phase.

Phase WMJ

[0077] The velocity criterion for the J phase is more distinct. In particular, (*t, x*) can only be assigned to the J phase if, both, up- and downstream of (*t, x*) low velocities are observed. Doing so ensures that WMJs are not extrapolated far beyond measurements in order to reduce wrongly estimated congested regions.

[0078] In order to efficiently compute this condition, measurements up- and downstream of (*t, x*) smoothing data with differing kernels are identified and the probabilities are computed independently. Then, the product of both probabilities represents the need to fulfill both requirements. Therefore, P_J^1 is computed as:

$$P_J^1(t,x) = \ \sigma\left(V_J^u(t,x), v_S^{thres}, \lambda_S\right) \cdot \ \sigma\left(V_J^d(t,x), v_J^{thres}, \lambda_J\right) \quad (13)$$

[0079] Where V_J^u and V_J^d denote the velocity fields computed as:

$$V_J^u(t,x) = V_{V_{FCD}}(w^0, \Phi_J^u, t, x) \quad (14)$$

$$V_J^d(t,x) = V_{V_{FCD}}(w^0, \Phi_J^d, t, x) \quad (15)$$

[0080] The different applied kernel functions Φ_J^u and Φ_J^d (see above) defined as:

$$\Phi_J^u(t,x) = \begin{cases} \Phi_{v_J^{dir}}^{\tau,\sigma}(t,x) \text{ if } x \le 0 \\ 0 \text{ else} \end{cases} \quad (16)$$

$$\Phi_J^d(t,x) = \begin{cases} \Phi_{v_J^{dir}}^{\tau,\sigma}(t,x) \text{ if } x \ge 0 \\ 0 \text{ else} \end{cases} \quad (17)$$

[0081] Note that Φ_J^u only considers data upstream of (*t, x*), Φ_J^d only considers data downstream of (*t, x*). In that way data are smoothed in different directions. The combination of the sigmoid functions of the velocities V_J^u and V_J^d ensures that WMJs are only reconstructed in between low velocity measurements. Note that eq. (13) uses different velocity thresholds v_J^{thres} and v_S^{thres} for the sigmoid functions. The difference stems from the expectation that once, due to downstream velocities below v_J^{thres} a WMJ is detected, this WMJ will propagate upstream as long as traffic upstream is in a state of critical flow-density (14). Since no density or flow data are available that state is assumed to be the congested region with the velocity threshold v_S^{thres}.

[0082] By requiring both criteria to be fulfilled it is ensured that the J phase is only reconstructed between low velocity measurements but never extrapolated. Possibly, the moving jam emerged earlier than the time the first equipped vehicle perceived it and propagated further upstream than the last equipped vehicle passing through the moving jam. However, sparse data does not allow to get to know exactly when the WMJ emerged and when it dissolved. Extrapolating a shockwave upstream or downstream means to risk overestimating it. Thus, this approach can be described as cautious aiming at minimizing wrongly estimated low velocities.

[0083] **Second** Class of Criteria P_p^2

[0084] The second criterion is a density criterion $P_p^2(t,x)$ that uses data density *D* (cf. equation (4) above) in order to quantify how well a phase hypothesis is supported by nearby data. This criterion enables coping with varying data density that comes along with FCD. Data density $D(w^0,\Phi_p,t,x)$ is computed for each phase $p \in \Omega$ with $\Omega = \{F,S,J\}$, using the respective kernel Φ_p. Since weighting w^0 and the applied kernels are greater than zero, also $D(w^0,\Phi_p,t,x)$ is always positive (or zero). In order to translate density into the probability P_p^D its values are limited to an upper bound of 1:

$$P_p^2(t,x) = \min\left(1, D\left(w^0, \Phi_p, t, x\right)\right) \tag{18}$$

[0085] In that way, P_p^2 equals to one if data is nearby, and converges to zero the greater the distance between (*t, x*) and the measurements. The validity of a measurement in space and time can be parametrized by adapting the kernel function or by modifying the weighting w^0.

Calculation of phase probabilities P_p' 222

[0086] The phase probabilities P_p' is the product of all phase criteria P_p^1 and P_p^2.

Calculation of uncertainty probability P_U 223

[0087] After calculating the phase probabilities P_p', the uncertainty $P_U(t, x)$ is calculated. P_U represents a probability that (*t, x*) does not belong to any of the phases:

$$P_U(t,x) = \Pi_{p\in\Omega}\left(1 - P_p{}'(t,x)\right) \tag{19}$$

[0088] Since in space-time (*t, x*) the uncertainty is high, a best-guess velocity $V_U(t, x)$ needs to be assumed. The speed limit is chosen in this example as best guess. However, it is clear to the skilled person that other kinds of velocities can be chosen as best guess, e.g. historical velocity averages. As outlined above, for the case where the uncertainty $P_U(t, x)$ is high, the best-guess velocity $V_U(t, x)$ is used as fallback-velocity that serves as best-guess velocity in case the uncertainty is high.

Dominance of J phase 224

[0089] As outlined above, the independent phase probabilities P'_P have been calculated. Since P'_p are independent, there exists an occurrence of regions, especially in the presence of shockwaves, where both, P'_J and P_S' or P'_F estimate high probabilities. This occurrence exists due to the different shapes of the convolution kernels and according velocities that are considered for the determination of each phase $\in \Omega$, *where* $\Omega = \{F,S,J\}$.

[0090] Since WMJs can propagate through other phases without interruption (14) and since the independent phase probabilities P'_J are supported by more distinctive criteria it is reasonable to assume that these regions rather belong to the J phase (phase J) than to any other one of the others phases p. Consequently, in those cases dominance of the J phase over the other phases is applied.

Final phase probabilities P_P 225

[0091] In view of the above, final phase probabilities P_P are set as:

$$P_J(t,x) = P_J{}'(t,x) \tag{20}$$

$$P_S(t,x) = P'_S(t,x) \cdot (1 - P_J(t,x)) \tag{21}$$

$$P_F(t,x) = P'_F(t,x) \cdot (1 - P_J(t,x)) \tag{22}$$

[0092] After the calculation of the final phase probabilities, now the velocities in space-time are calculated 230

[0093] Phase-dependent velocity estimates $V_p^H(t,x)$ 231

[0094] As outlined above, the raw trajectory data 210 was taken in order to calculate the appropriate traffic phases p in space and time using characteristic smoothing kernels and several criteria that allow distinguishing between them.

[0095] Now, the calculated traffic phases p are taken to accurately calculating the traffic velocities. The traffic phases enable determining a region in space and time a velocity measurement has validity. For example, a low velocity measurement that is part of a Wide Moving Jam allows estimating the mean velocity of all vehicles that are part of the Wide Moving Jam. However, it does not enable a determination about a traffic velocity in an adjacent free flow or synchronized flow phase.

[0096] The calculation of phase-dependent velocities V_p^H is performed as follows:

$$V_p^H(t,x) = \frac{1}{V_{V_{FCD}^{-1}}(P_p, \Phi_p^H, t, x)} \tag{23}$$

[0097] Where $V_{V_{FCD}^{-1}}(\mathrm{P_p}, \Phi_\mathrm{p}^\mathrm{H}, \mathrm{t}, \mathrm{x})$ denotes the convolution process (cf. equation (5)) smoothing the *inverted* trajectory velocities $V_{V_{FCD}^{-1}}$ with the convolution kernel Φ_p^H. In this example, for numerical reasons, a minimal velocity of 3*km/h* is assumed. This enables that the smoothing process resembles a harmonic mean instead of an arithmetic one, which accounts for precision in travel time reconstruction (cf. equation (24)).

[0098] In addition, instead of a normal weighting w^0 as used in the smoothing for calculating the phase probabilities 220, the final phase probabilities P_p are used as weights for the input data.

[0099] In other words, for the computation of each V_p^H mostly those measurements are taken into account that belong to phase *p*. Note that convolution kernels Φ_p^H can be parametrized differently from the convolution kernels Φ_p. The reason is that the shapes of Φ_p account for the characteristic propagation of phases, such as the propagation of J phases upstream and the stationary character of S phases. Φ_p^H, on the other hand influence how data inside an already identified phase is smoothed, where data is weighted with respect to the final phase probabilities P_p. A distinction between the parameters for example enables the reconstruction of a stationary synchronized flow phase with a large isotropic kernel Φ_S and subsequently estimating velocities inside the phase with a smaller anisotropic kernel Φ_S^H that reconstructs minor shockwaves (narrow moving jams (14)) occurring inside the phase.

Aggregation of probabilities and velocities into a final velocity estimate V_E 232

[0100] Finally, the phase probabilities *Pp* and respective velocities V_p^H are estimated. Additionally, probability P_U is computed and *best-guess* velocity V_U is assumed. For aggregating all velocities and probabilities into a final velocity estimate V_E, a weighted average is applied:

$$V_E(t,x) = \frac{P_U(t,x) \cdot V_U(t,x) + \sum_{p \in \Omega} P_p(t,x) \cdot V_p^H(t,x)}{P_U(t,x) + \sum_{p \in \Omega} P_p(t,x)} \tag{24}$$

EVALUATION

[0101] To prove the accuracy of the above-mentioned approach for estimating traffic speed, a study was conducted with sparse FCD. To do so, real FCD collected during a traffic jam on German freeway A99 on the 15th July, 2014, were used. First, available data and discretization of the approach are briefly described. Then, resulting probabilities and velocities applying the above are illustrated. Finally, the accuracy of the traffic speed estimation is compared to two other algorithms that are less accurate.

[0102] Available sparse FCD consist of timestamps and GPS positions sampled anonymously by individual vehicles with sampling times between 20s and 30s. An installed filter in the processing unit of the equipped vehicles retains packages of data, wherein each package of data contains a plurality of FCD for covering the case that, the vehicle's velocity does not match an expected velocity. The expected velocity is a state machine that is influenced by individually recorded velocities and provided velocity estimates. The results are fractions of complete trajectories being reported, with the positive result that individuals cannot be tracked along their journey. That filter mechanism was introduced to ensure each driver's privacy. Still, in case of congestion, detailed velocity data was collected. **Figure 4** shows raw trajectory data 210 for a road segment 420, 430 (i.e. the congestion on German highway A99 direction north) are displayed. The triangles 440 mark positions of on- and off-ramps along the road segment 420, 430.

[0103] The pattern shows different characteristics often occurring in congested freeway traffic. As can be seen, around 7:45am, a moving jam phase emerged that evolved into a WMJ and induced a traffic breakdown at the on-ramp at position 10 km. The WMJ propagated further upstream and induced another traffic breakdown at a neighboring bottleneck. The pattern evolves into a General Pattern (GP) expanding over two bottlenecks where the downstream fronts of synchronized flow phases are fixed slightly downstream the on-ramp positions. In the pinch zone of the downstream synchronized flow phase a few WMJs originate and propagate upstream.

Discretization

[0104] In order to apply estimation methods, time and space dimension are discretized into intervals of length ΔL = 50*m* and ΔT = 10*s* called grid cells. Average velocities between GPS positions and respective timestamps are computed and the grid cells the vehicle occupies are determined. Then, each trajectory $c = 1,..., N_c$ is written as a set of tuples $r = \{(t,x,v,w)_1,..., (t,x,v,w)_{n_{tr}}\}$ where each tuple represents the mean velocity of the vehicle at space-time *(t, x)* referring to the center of the grid cell in space and time, and weight *w* E [0,1] is used to mark the part of the cell that is occupied by the vehicle. If two velocities of different trajectories are assigned to the same cell, their mean value is determined and the weights *w* are added. The discretization of the approach requires to discretize the continuous 2D convolution. An efficient implementation of the discrete 2D convolution can be performed e.g. using the Fast Fourier Transform.

[0105] **Figure 5** depicts the computation of the final phase probabilities P_P (P_J, P_S and P_F) 510 computed with all available trajectories. Based on the final phase probabilities P_P 510, for each phase p, a phase velocity V_p^H is computed

520. Finally, the velocity estimate V_E 530 is shown. Next to V_E 530, the probability (1 - P_U) 540 is depicted that can be interpreted as quality value, where a value of one means high and a value of zero means low certainty of the result.

Evaluation of accuracy

[0106] For an objective evaluation of the accuracy of the calculated velocities, a comparison with other algorithms was performed. For comparison, two common approaches that do not require density or flow data are taken into consideration. The first approach is the Generalized Adaptive Smoothing Method (GASM) that is based on the observation that shockwaves in congested traffic propagate upstream and shockwaves in free traffic propagate downstream. Here, the GASM is applied as described in "Treiber, M., and D. Helbing: An adaptive smoothing method for traffic state identification from incomplete information. Interface and Transport Dynamics, Vol. 32, 2003, pp. 343-360" (Treiber) and van Lint, J. Empirical Evaluation of New Robust Travel Time Estimation Algorithms. Transportation Research Record: Journal of the Transportation Research Board, 2160, 2010, pp. 50-59" with an adaption to sparse FCD. The adaption describes how sparse FCD and a best-guess velocity can be fused in order to provide a continuous velocity estimate if no data is nearby. The weighting ratio of FC data to the velocity fallback is 1000:1. Parametrization is chosen according to Treiber. Further, an isotropic smoothing approach (naïve approach) is applied that smooths data mostly in time and slightly in space.

[0107] Applied PSM parameters are listed in Table 2. The velocity thresholds v_p^{thres} were explained above, the propagation directions v_p^{dir} have been set similar to Treiber. The other parameters which are mainly the sizes of the kernels Φ_p and Φ_p^H have been set with respect to typically observed properties of congestion: WMJs often have a higher spatial than temporal extent, thus σ_J is greater than τ_J. Synchronized flow phases are rather stationary or, if not, their downstream fronts usually stick to adjacent upstream bottlenecks and remain there. Thus, the kernel has a relatively high value τ_S compared to σ_S, which results in a larger temporal smoothing. Kernel Φ_S^H, which is applied after identifying the S phase, is smaller in time but larger in space. Effectively, minor shockwaves are propagated correctly upstream. The kernels for the free flow phase are medium sized. In experiments, estimation accuracies were less sensitive to changes of these parameters.

Table 2: Parameters for the presented approach (PSM)

Parameter \ Phase	J	S	F
τ_p	20s	300s	150s
σ_p	500m	50m	100m
v_p^{dir}	-18 km/h	0 km/h	70 km/h
v_p^{thres}	30 km/h	65 km/h	55 km/h
λ_p	0.4 h/km	0.5 h/km	0.5 h/km
τ_p^H	20s	100s	150s
σ_p^H	500m	200m	100m
$v_p^{dir,H}$	-18 km/h	-18 km/h	70 km/h

Results

[0108] In the following, estimation accuracy of the PSM, the GASM and the naïve approach are compared qualitatively and quantitatively. Since data density has the most significant impact on the accuracy of the result, for both comparisons this parameter is varied.

Qualitative results

[0109] **Figure 6** shows the obtained estimation results applying the three approaches (PSM, GASM, naïve) with limited data coverage, i.e. sparse FCD 610. As can be seen in plot 620, the naïve approach manages to estimate the stationary traffic upstream the two bottlenecks well but fails in reconstructing moving jams. It smooths the low velocities that actually propagate upstream in temporal direction only, such that the estimation of the congestion pattern s is inaccurate.

[0110] As can be seen in Plot 630, the GASM-approach manages to reconstruct the moving jams more accurately than the naïve approach, however, also here the estimation of velocities is wrong for many grid cells. For example, the latest moving jam is extrapolated further upstream than it actually propagated. Furthermore low velocities are smoothed slightly beyond the downstream bottleneck at kilometer 10. Further, the queueing traffic at the bottlenecks are not accurately estimated. Zones that are actually in congested state are estimated as free flow.

[0111] The PSM-approach manages to accurately distinguish between the queueing traffic at the bottlenecks and the WMJs. The gaps in data that belong to moving jams are correctly classified as J phase and respective low velocities are estimated. Gaps in the stationary traffic upstream the bottlenecks are accurately reconstructed as synchronized flow phases such that appropriate velocities are estimated from data in the same phase. An expected estimation failure occurs at 8:00am where the moving synchronized flow is treated as stationary congestion and velocities are smoothed in temporal direction. That improves as the velocities drop further and a J phase is identified. Comparing the reconstruction quality of moving jams calculated by the PSM approach and the GASM approach, estimated phase fronts by the PSM have sharper edges. This improved accuracy is very valuable feature for using the fronts for predictions in a navigation system and/or hazard warnings, especially for autonomous driving.

Quantitative results

[0112] In order to evaluate an algorithm quantitatively, the set of N_c trajectories is divided into a training set and a test set. The training set is used in order to estimate velocities V_E, and the test set is used to evaluate the accuracy of that estimate. The size $N_T \in \mathbb{N}$, $0 < N_T < N_c$ of the test set T_T is defined as:

$$N_T = \alpha N_c \tag{25}$$

[0113] With $\alpha \in]0,1[$.The size N_E of the training (estimation) set is the $(1 - \alpha)$ part of all trajectories. Additionally, that part is varied with another factor $\beta \in]0,1[$that is used in order to simulate different data densities:

$$N_E = \beta(1 - \alpha)N_c \tag{26}$$

[0114] For the sake of interpretation, N_E is normalized with the analyzed time interval T, resulting in the data density δ_E:

$$\delta_E = \frac{N_E}{T} \tag{27}$$

[0115] Then, δ_E denominates the number of trajectories per hour that are used for the estimation process.

[0116] There exists a variety of quality measures. Since a deviation between estimate and ground truth is more critical in congested regimes than in free flow, here the Mean Absolute Percentage Error (MAPE) is applied as metric:

$$MAPE_{V_E} = \frac{1}{n_{test}} \sum_{tr \in T_T} \sum_{(t,x,v) \in tr} \left| \frac{V_E(t,x) - v}{v} \right| \tag{28}$$

[0117] Where $T_T = \{tr_1, tr_2, \ldots, tr_{N_T}\}$ denotes the test set of trajectories tr, and $n_{test} \in \mathbb{N}_+$ the total number of tuples in all test trajectories $tr \in T_T$:

$$n_{test} = \sum_{tr \in T_T} |T_T| \tag{29}$$

[0118] **Figure 7** shows the MAPE with respect to data densities δ_E between 10 traces/hour and 90 traces/hour for the naïve approach 710, the GASM approach 720 and the PSM approach 730. The presented error values are the mean MAPE of 50 iterations with randomly assigned training and test set in order to ensure robustness of the results.

[0119] The results show that all approaches achieve more accurate results with higher data densities. However, the gain using the naïve approach is significantly lower than the gain achieved by the GASM approach, which itself is significantly lower than the gain achieved by the PSM approach. Compared to the other two approaches, the PSM-approach shows the lowest error values for all data densities and thus, can be entitled as the most accurate algorithm.

Claims

1. Computer system for calculating accurate estimations of traffic velocity in a road network, the system comprising:

   a plurality of devices, each device operable to deliver speed measurement data (210) corresponding to the speed of a traffic flow in the road network; and
   at least one computational unit,
   wherein each of the plurality of devices sends speed measurement data (210) to the computational unit, and
   wherein the computational unit is operable to calculate accurate estimations of traffic velocity in the road network by:

   - identifying (220) regions with varying sizes and moving boundaries under the condition that within each region, a corresponding traffic phase p is constant, wherein each traffic phase is one of a free-flow phase, a synchronized phase or a wide moving jam phase; and
   - calculating (230) accurate estimations of traffic velocity in said regions based on the corresponding traffic phases.

2. System according to claim 1, wherein each speed measurement data (210) comprises at least a location of a vehicle driving on the road network and a corresponding timestamp; and
   wherein each speed measurement data (210) may further comprise:

   - a velocity of the vehicle at a point in time corresponding to the timestamp;
   - a direction of the vehicle at the point in time corresponding to the timestamp;
   - a lane the vehicle is driving on; and/or

   data on vehicles and their velocities surrounding the vehicles.

3. System according to any one of the preceding claims, wherein the identifying (220) of the regions comprises:

   - calculating (221), from the speed measurement data (210), criteria probabilities $P_p^i(t,x)$ for each traffic phase p;
   - calculating (222), as the product of all criteria probabilities, the independent probability independent probability $P'_p(t,x)$ for each traffic phase p;
   - estimating (223) the uncertain probability $P_U \in [0,1]$, wherein P_U describes a level of uncertainty in assigning (t, x) to any of the phases p;
   - taking (224) into account the dominance of the wide moving jam phase; and
   - determining (225) final phase probabilities *Pp*;

   wherein P denotes probability; and p denotes phase.

4. System according to claim 3, wherein calculating (221) criteria probabilities P_p^i comprises the following:

   let $P_p^1, P_p^2, \dots, P_p^{N_k}$, $P_p^i \in \mathbb{R}$ be $N_k(p) \in \mathbb{N}\backslash\{0\}$ criteria that (t, x) needs to fulfill in order to belong to phase p. Each criterion is modelled as a fuzzy decider $P_p^i \in [0,1]$.

5.

System according to claim 3 or claim 4, wherein the independent probability $P_p'(t,x)$ for each traffic phase p is calculated as follows:

$$P_p'(t,x) = \prod_i^{N_k(p)} P_p^i(t,x).$$

6. System according to any one of claims 3 to 5, wherein the uncertain probability $P_U \in [0,1]$ describes the probability that *(t, x)* does not belong to a phase is calculated by:

$$P_U(t,x) = \Pi_{p\in\Omega}\left(1 - P_p{}'(t,x)\right)$$

7. System according to any one of claims 3 to 6, wherein:

if there is an occurrence of a high probability of a region belonging to (P_J' and (P_S' or P_F')):

taking (224) into account the dominance of P_J'.

8. System according to claim 7, wherein determining (225) the final phase probabilities P_p while taking into account the dominance of P_J' for each region is performed as follows:

$$P_J(t,x) = P_J{}'(t,x)$$

$$P_S(t,x) = P_S'(t,x) \cdot (1 - P_J(t,x))$$

$$P_F(t,x) = P_F'(t,x) \cdot (1 - P_J(t,x)).$$

9. System according to any one of the preceding claims, wherein calculating (230) accurate estimations of traffic velocity based on a prevailing traffic phase in the road network comprises:

estimating (231) phase-dependent velocity estimates $V_p^H(t,x)$; and

aggregating (232) final-phase probabilities P_p and corresponding velocity estimates $V_p^H(t,x)$ into velocity estimates V_E.

10. System according to claim 9, wherein estimating (231) phase-dependent velocity estimates $V_p^H(t,x)$ is performed as follows:

$$V_p^H(t,x) = \frac{1}{V_{V_{FCD}^{-1}}(P_p, \Phi_p^H, t, x)};$$

with $V_{V_{FCD}^{-1}}(\mathrm{P_p}, \Phi_\mathrm{p}^\mathrm{H}, \mathrm{t}, \mathrm{x})$ denotes a convolution process smoothing the inverted trajectory velocities $V_{V_{FCD}^{-1}}$ with the convolution kernel Φ_p^H.

11. System according to claim 9 or claim 10, wherein aggregating (232) final-phase probabilities P_p and the corresponding velocity estimates $V_p^H(t,x)$ into velocity estimates V_E comprises:

$$V_E(t,x) = \frac{P_U(t,x)\cdot V_U(t,x)+\sum_{p\in\Omega} P_p(t,x)\cdot V_p^H(t,x)}{P_U(t,x)+\sum_{p\in\Omega} P_p(t,x)};$$

with V_U = a speed limit of the respective region.

12. System according to any one of the preceding claims, wherein at least one vehicle driving on the road network supports an autonomous driving mode;
wherein the computational unit is further operable to send the accurate estimations of traffic velocity to the vehicle supporting the autonomous driving mode; and
wherein the vehicle supporting the autonomous driving mode is operable to take the accurate estimations of traffic velocity into account when operating in the autonomous driving mode.

13. Computer-implemented method for calculating accurate estimations of traffic velocity in a road network, the method comprising:

sending, by a plurality of devices, speed measurement data (210) to a computational unit, wherein each speed measurement data corresponds to the speed of a traffic flow in the road network, and
calculating, by the computational unit, accurate estimations of traffic velocity in the road network by:

- identifying (220) regions with varying sizes and moving boundaries under the condition that within each region, a corresponding traffic phase p is constant, wherein each traffic phase is one of a free-flow phase, a synchronized phase or a wide moving jam phase; and
- calculating (230) accurate estimations of traffic velocity in said regions based on the corresponding traffic phases.

14. Computer program product comprising instructions thereon, which, when loaded and executed by at least one processor, cause the at least one processor to perform a method according to claim 13.

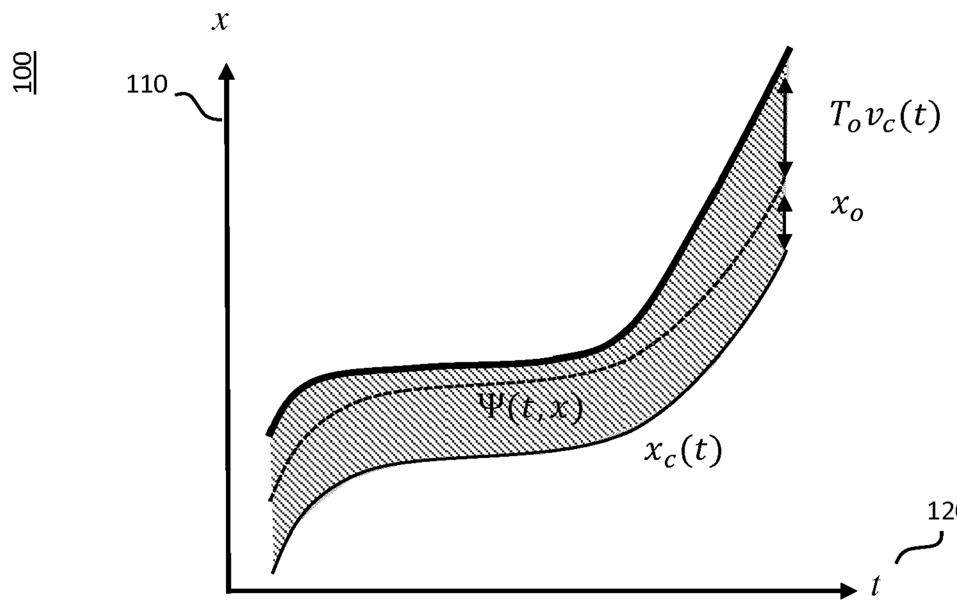

Fig. 1A

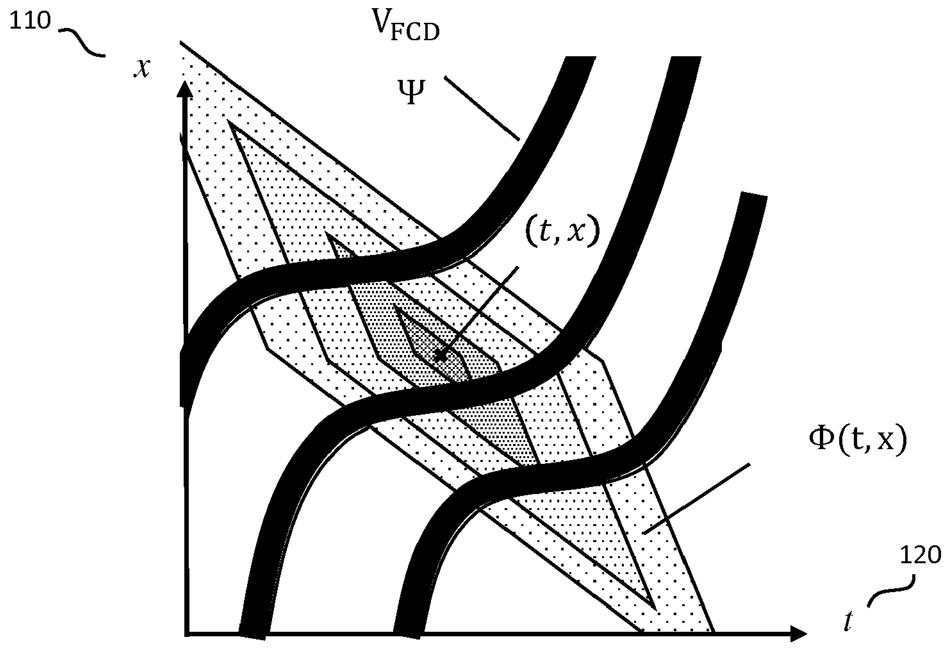

Fig. 1B

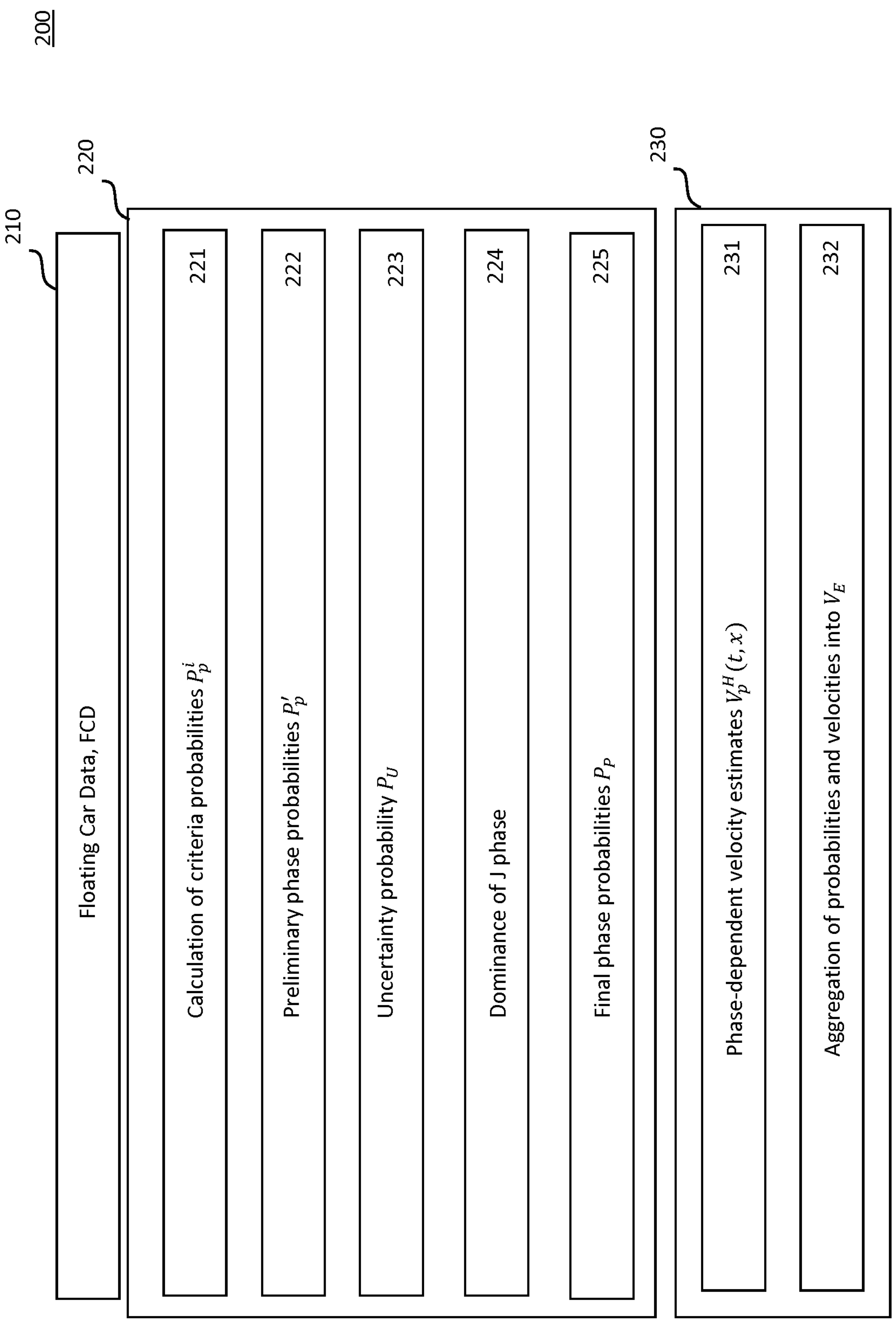
200
210
Floating Car Data, FCD
220
221
Calculation of criteria probabilities P_p^i
222
Preliminary phase probabilities P'_p
223
Uncertainty probability P_U
224
Dominance of J phase
225
Final phase probabilities P_P
230
231
Phase-dependent velocity estimates $V_p^H(t,x)$
232
Aggregation of probabilities and velocities into V_E

Fig. 2

300

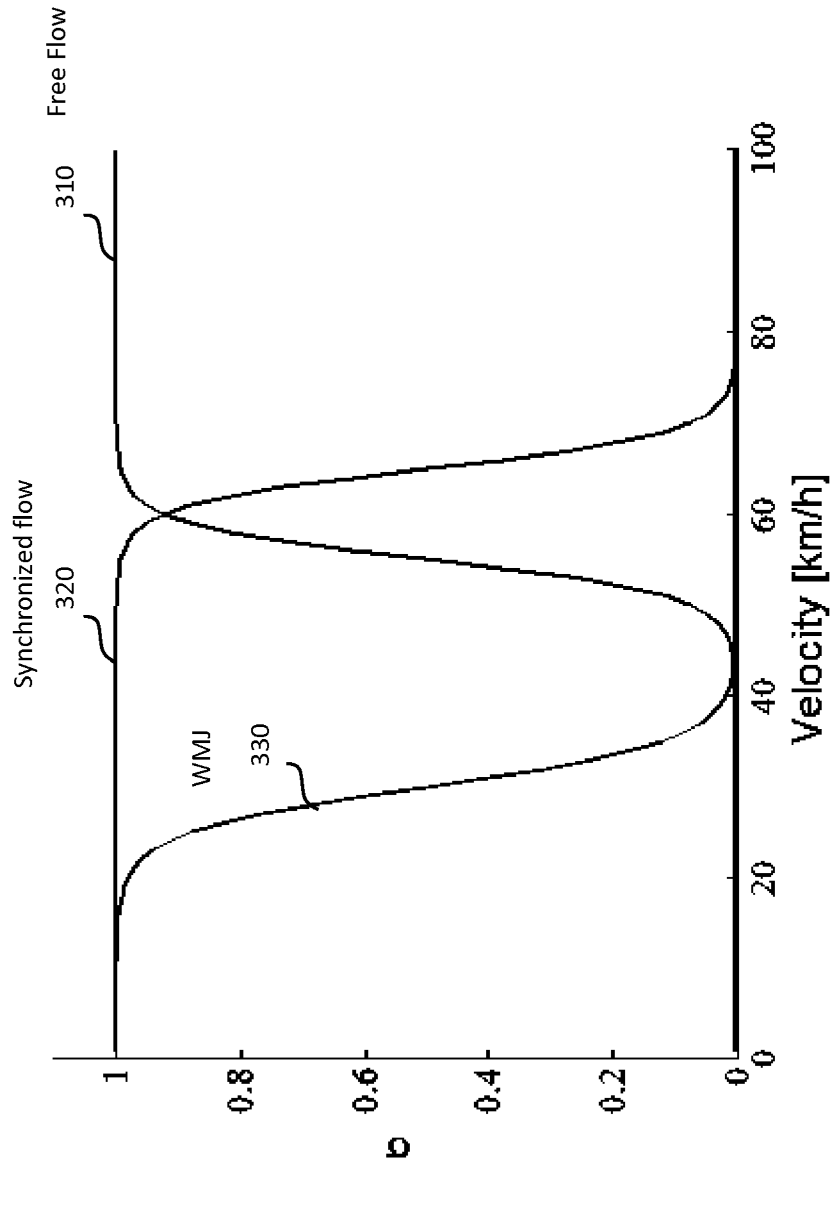
Free Flow
310
Synchronized flow
320
WMJ
330
σ
1
0.8
0.6
0.4
0.2
0
0
20
40
60
80
100
Velocity [km/h]

Fig. 3

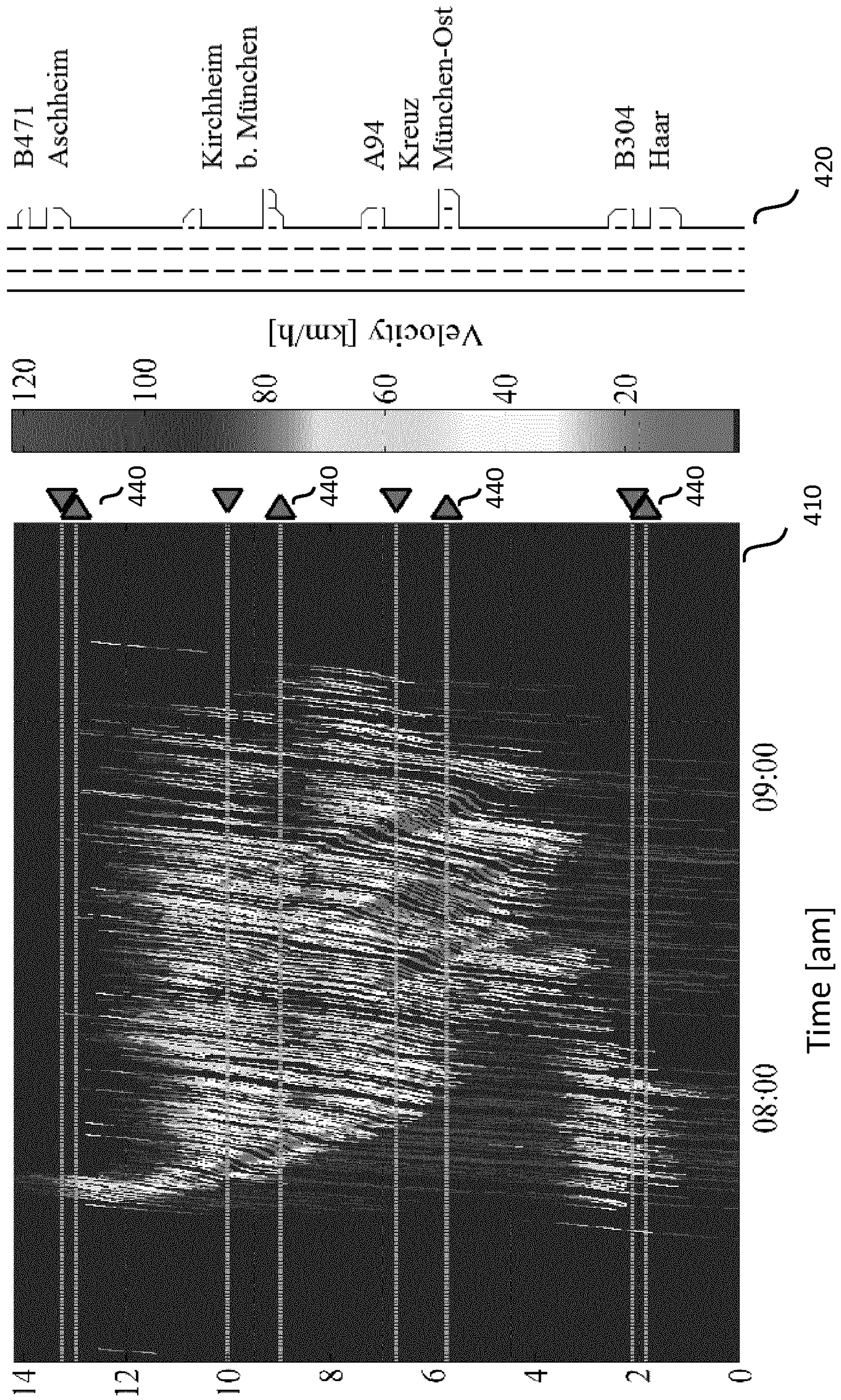
B471
Aschheim
Kirchheim
b. München
A94
Kreuz
München-Ost
B304
Haar
420
Velocity [km/h]
120
100
80
60
40
20
440
440
440
440
410
Position [km]
14
12
10
8
6
4
2
0
08:00
09:00
Time [am]

Fig. 4

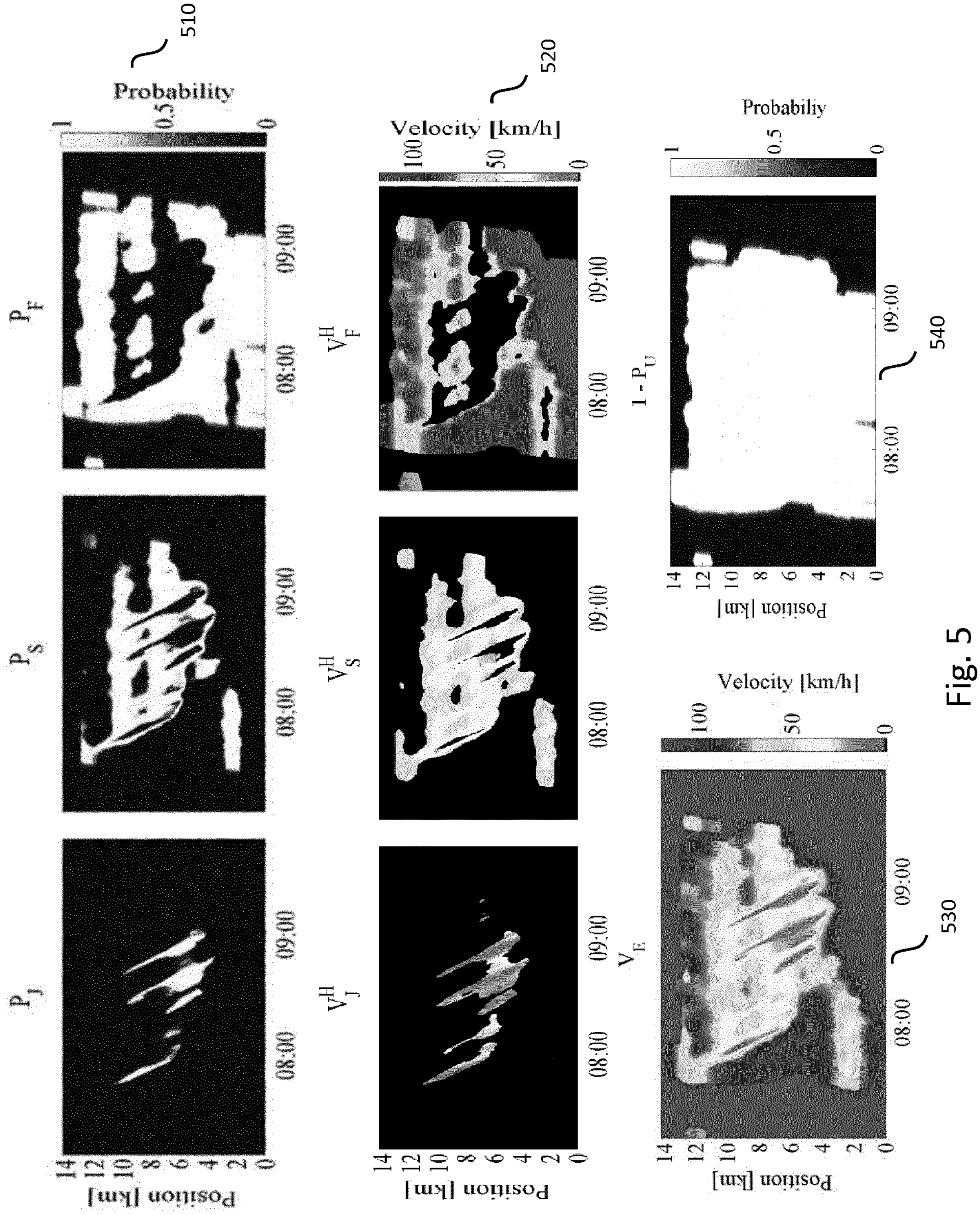
510
520
530
540
P_J
P_S
P_F
V_J^H
V_S^H
V_F^H
V_E
$1 - P_U$
Probability
Probabiliy
Velocity [km/h]
Position [km]
08:00
09:00

Fig. 5

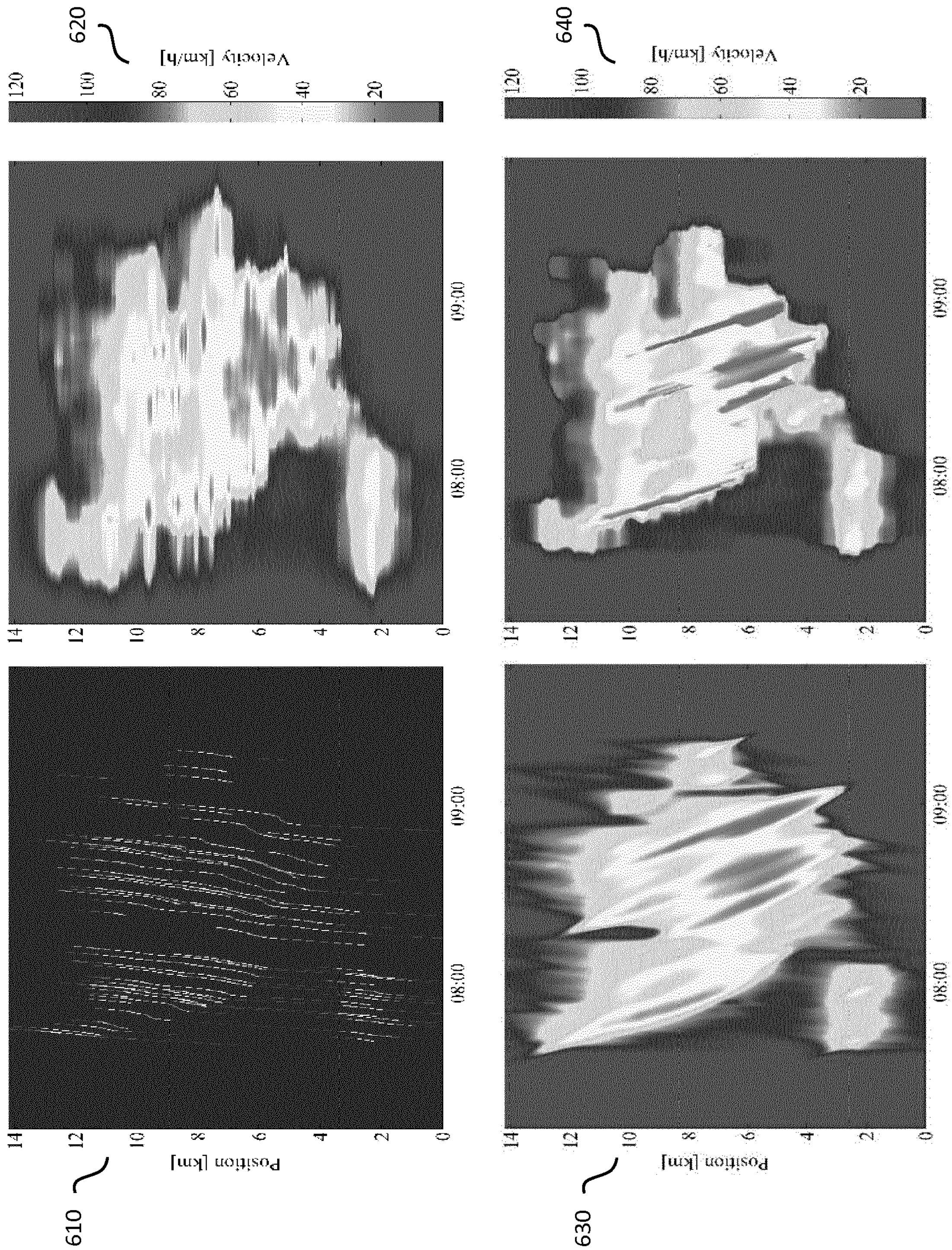

Fig. 6

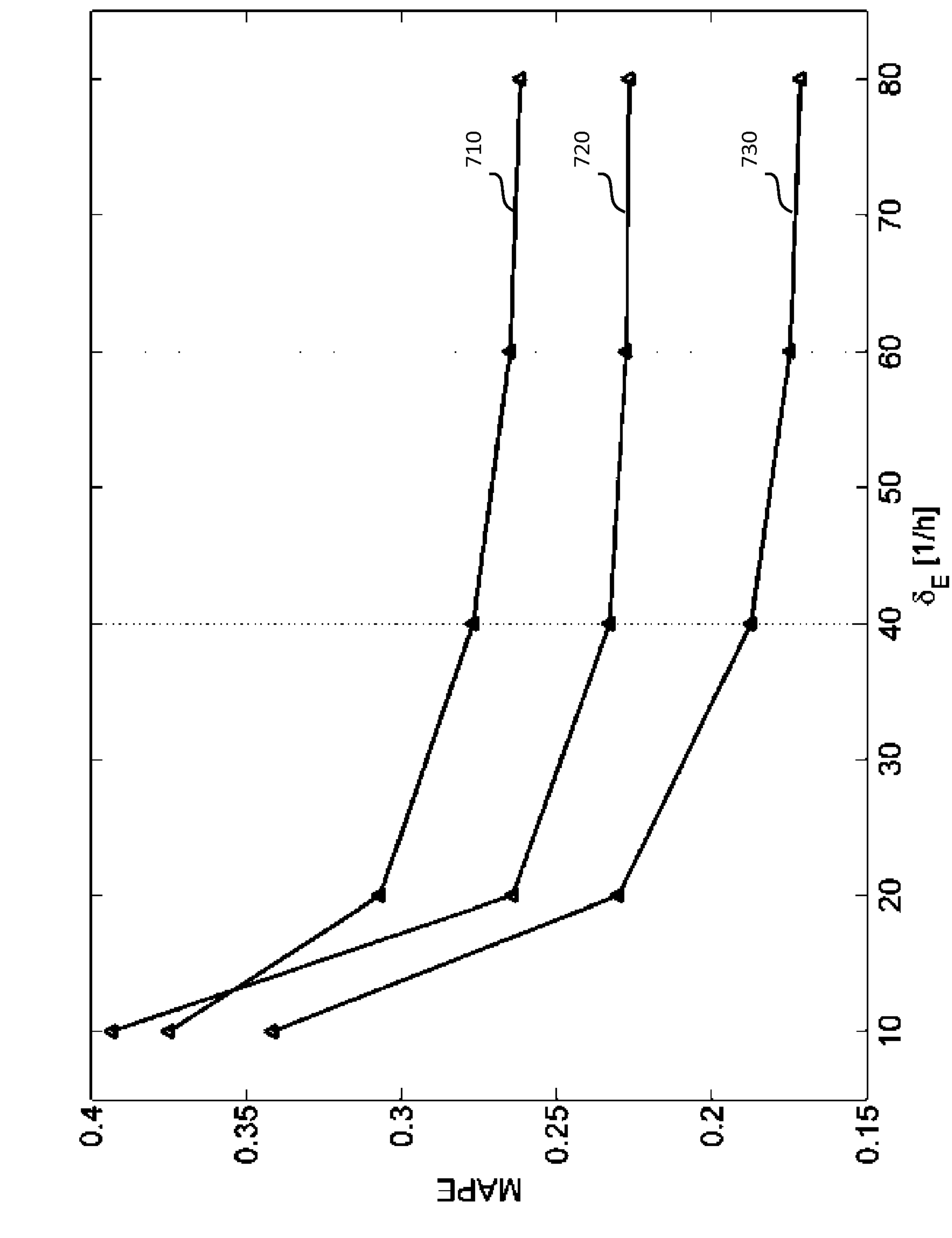

Fig. 7

Europäisches Patentamt
European Patent Office
Office européen des brevets

EUROPEAN SEARCH REPORT

Application Number
EP 16 20 5483

DOCUMENTS CONSIDERED TO BE RELEVANT

Category	Citation of document with indication, where appropriate, of relevant passages	Relevant to claim	CLASSIFICATION OF THE APPLICATION (IPC)
X	US 2016/071411 A1 (STENNETH LEON OLIVER [US]) 10 March 2016 (2016-03-10) * abstract * * paragraph [0030] - paragraph [0031] * * paragraph [0047] - paragraph [0051] * * claims 1, 3, 5, 10 * -----	1-14	INV. G08G1/01 G08G1/0967
X	REMPE FELIX ET AL: "Online Freeway Traffic Estimation with Real Floating Car Data", 2016 IEEE 19TH INTERNATIONAL CONFERENCE ON INTELLIGENT TRANSPORTATION SYSTEMS (ITSC), IEEE, 1 November 2016 (2016-11-01), pages 1838-1843, XP033028589, DOI: 10.1109/ITSC.2016.7795854 [retrieved on 2016-12-22] * the whole document * -----	1-14	
X	MARTIN TREIBER ET AL: "An adaptive smoothing method for traffic state identification from incomplete information", ARXIV.ORG, CORNELL UNIVERSITY LIBRARY, 201 OLIN LIBRARY CORNELL UNIVERSITY ITHACA, NY 14853, 2 October 2002 (2002-10-02), XP080097270, * the whole document * -----	1-14	TECHNICAL FIELDS SEARCHED (IPC) G08G

The present search report has been drawn up for all claims

1

Place of search	Date of completion of the search	Examiner
The Hague	29 May 2017	Renaudie, Cécile

CATEGORY OF CITED DOCUMENTS

X : particularly relevant if taken alone
Y : particularly relevant if combined with another document of the same category
A : technological background
O : non-written disclosure
P : intermediate document

T : theory or principle underlying the invention
E : earlier patent document, but published on, or after the filing date
D : document cited in the application
L : document cited for other reasons

& : member of the same patent family, corresponding document

EPO FORM 1503 03.82 (P04C01)

ANNEX TO THE EUROPEAN SEARCH REPORT ON EUROPEAN PATENT APPLICATION NO. EP 16 20 5483

This annex lists the patent family members relating to the patent documents cited in the above-mentioned European search report. The members are as contained in the European Patent Office EDP file on
The European Patent Office is in no way liable for these particulars which are merely given for the purpose of information.

29-05-2017

Patent document cited in search report	Publication date	Patent family member(s)	Publication date
US 2016071411 A1	10-03-2016	NONE	

EPO FORM P0459

For more details about this annex : see Official Journal of the European Patent Office, No. 12/82

REFERENCES CITED IN THE DESCRIPTION

This list of references cited by the applicant is for the reader's convenience only. It does not form part of the European patent document. Even though great care has been taken in compiling the references, errors or omissions cannot be excluded and the EPO disclaims all liability in this regard.

Non-patent literature cited in the description

- **TREIBER, M. ; D. HELBING.** An adaptive smoothing method for traffic state identification from incomplete information. *Interface and Transport Dynamics,* 2003, vol. 32, 343-360 **[0106]**
- **VAN LINT, J.** Empirical Evaluation of New Robust Travel Time Estimation Algorithms. *Transportation Research Record: Journal of the Transportation Research Board,* 2010, vol. 2160, 50-59 **[0106]**